DELAYED HYDRIDE CRACKING AND ELASTIC PROPERTIES OF EXCEL, A CANDIDATE CANDU-SCWR PRESSURE TUBE MATERIAL

Z.L. Pan
Atomic Energy of Canada Limited, Chalk River Laboratories,
Chalk River, Ontario, Canada, K0J 1J0

Abstract

Excel, a Zr alloy which contains 3.5%Sn, 0.8%Nb and 0.8%Mo, shows high strength, good corrosion resistance, excellent creep-resistance and dimension stability and thus is selected as a candidate pressure tube material for CANDU-SCWR. In the present work, the delayed hydride cracking properties (K_{IH} and the DHC growth rates), the hydrogen solubility and elastic modulus were measured in the irradiated and unirradiated Excel pressure tube material.

1. Introduction

The fuel channel design of CANDU® reactors can be adapted to use supercritical water as the coolant. With this modification the thermodynamic efficiency of the reactor is increased to over 40% [1]. In addition, the CANDU-Supercritical Water Reactor (SCWR) offers advantages over other designs in terms of increased sustainability, improved economic performance, safety, reliability and resistance to proliferation of non-peaceful applications of nuclear energy [1]. The Generation-IV International Forum (GIF) [2] has considered the SCWR as one of the six Gen-IV nuclear reactor concepts because of these advantages.

Similar to the current CANDU reactor design, the CANDU-SCWR is moderated using heavy water and has fuel bundles residing inside horizontal fuel channels. The coolant, however, is light water, operating at supercritical conditions with a pressure of 25 MPa, an inlet temperature of 350°C and an outlet temperature of 625°C [3,4]. AECL has proposed a preliminary design for the CANDU-SCWR fuel channel, termed the High Efficiency Channel (HEC) [3-6]. Unlike the current CANDU fuel channel, the HEC does not use a calandria tube to separate the pressure tube from the moderator, which operates at an average temperature of ~80°C [3,4]. The pressure tube is thermally isolated from the hot coolant by a porous ceramic insulator tube, as shown in Fig. 1. A perforated metal liner tube protects the insulator tube from being damaged by the fuel bundles and from erosion by the coolant flow. The coolant pressure is transmitted to the pressure tube through small openings in the insulator and the liner. Because the moderator is in contact with the pressure tubes, their operating temperatures of ~100°C allow the use of Zr alloys. Detailed properties of the Zr alloy are required for the design of the HEC.

A Zr alloy, developed by AECL in 1970s – 1980s and termed Excel, has a high strength and high creep resistance [7-10]. Zr alloy Excel contains 3.5% Sn, 0.8% Nb and 0.8% Mo and its heat treatment includes a vacuum anneal at 740°C for 0.5 hr, a vacuum cool and an autoclave at

® CANDU is a registered trademark of Atomic Energy of Canada Limited (AECL).

400°C for 24 hr. The annealed Excel was selected as a candidate pressure tube material for the HEC design [3,4]. There is little information of the delayed hydride cracking (DHC) growth rates for either unirradiated or irradiated Excel at temperatures corresponding to the operating conditions for a pressure tube in the HEC design. When the hydrogen concentration in a pressure tube exceeds the solubility, hydrides will precipitate and the tube would be susceptible to DHC, thus the hydrogen solubility in Excel is also required to determine. Goals for the present work include:

(1) measuring the DHC growth rates in the axial and radial directions for both unirradiated and irradiated Excel pressure tube material at temperatures from 80 to 130°C;

(2) determining the radial-axial threshold stress intensity factor K_{IH} for DHC in both unirradiated and irradiated Excel materials at 100°C;

(3) measuring the terminal solid solubility (TSS) of hydrogen at lower temperatures in irradiated and unirradiated Excel specimens; and

(4) measuring the elastic modulus of unirradiated Excel as a function of temperature.

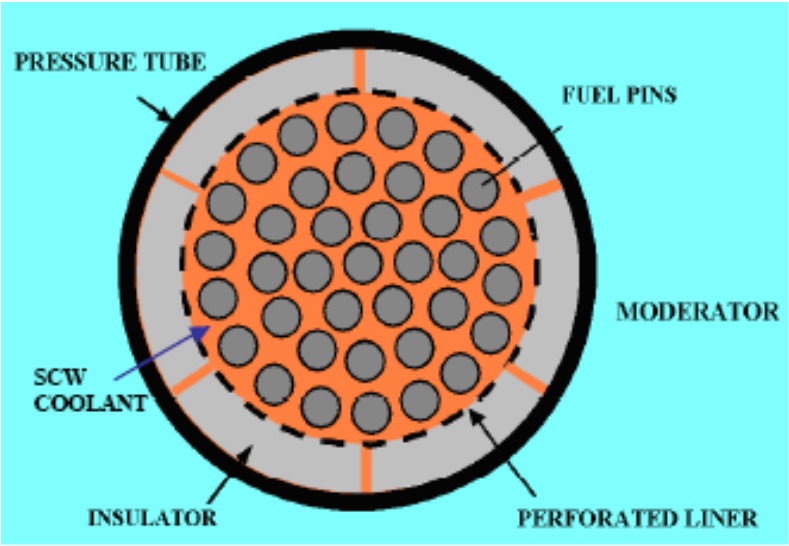

Fig. 1 A preliminary design of the High Efficiency Channel (HEC) for the CANDU–SCWR [3].

2. Experiments

2.1 Material and specimen geometry

For this investigation, all Excel specimens were machined from pressure tubes #600 and #601. Both tubes were manufactured in the early 1980s and are in the annealed condition. Details of the manufacturing route are outlined in [7-10]. Tube #601 is unirradiated but tube #600 was

irradiated in the NRU reactor at Chalk River Laboratories. Tube #600 was placed in the U2 loop of the NRU reactor as a pressure tube at the hot leg of assembly ID #50210 from 1982 to August 1991. The central section of this pressure tube was located in the reactor core, where the received neutron fluence was 2.8 x 10^{25} n/m^2 (E>1 MeV) at an average temperature of 285°C.

Cantilever Beam (CB) specimens with a length of 38 mm or 19 mm in the circumferential direction, as shown in Fig. 2, were used for K_{IH} tests and DHC growth rate tests in the radial direction. Twelve 38 mm long and four 19 mm long CB specimens were machined from tube #601 at ~0.3 m from the front end of the tube, i.e. the front side of the extruded tube. The centre notch for the unirradiated specimens was 0.5 mm deep with a root radius of ~15 μm. For the DHC growth rate tests in the axial direction, eight Curved Compact Toughness (CCT) specimens were used, Fig. 2. These CCT specimens were pre-cracked by fatigue cycling at room temperature to produce an initial relative crack length of a/W ≈ 0.5.

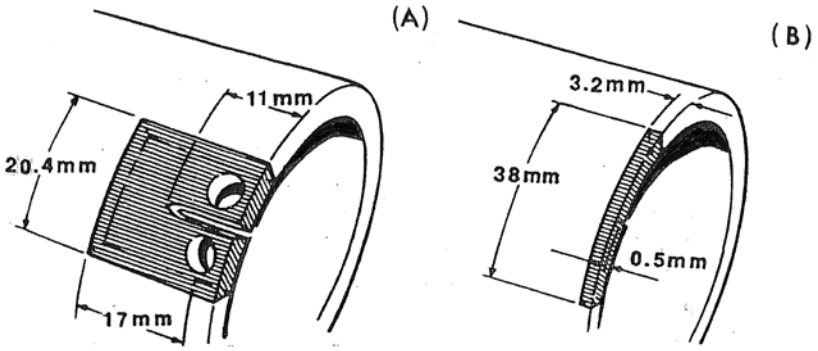

Fig. 2 Schematic diagrams of CCT specimen (A) and CB specimen (B), dimensions in mm.

Irradiated specimens were machined from a 38 cm section of tube #600, located 6.14 m from the top of pressure tube assembly #50210, i.e. at the middle of the reactor core. From the tube, 19 mm long CB specimens were machined. The specimens were broached with a notch 0.5 mm deep with a root radius of ~ 5 μm. All irradiated specimens were tested with the original hydrogen concentration of ~ 20μg/g. For TSS measurements, three coupons were cut from an irradiated CB specimen #1846-5 using a slow speed saw and the original surfaces of specimens were retained.

2.2 DHC growth rate tests

DHC growth rates in the axial direction, denoted DHCVa, were measured on CCT samples. DHC growth rates in the radial direction, denoted DHCVr, were measured on CB specimens. The test procedures are outlined in [11-13]. For these tests the peak temperature of 280°C was selected to be in the range of irradiation temperature experienced for pressure tube #600. Each specimen was held at the peak temperature for 1 hour before cooling to the test temperature at 1°C/min. The specimen was then held for half an hour before a load was applied by a computer controlled stepping motor to produce a nominal stress intensity factor of 15 MPa√m at the crack tip. Crack initiation was detected using the elastic compliance method, which is different from the acoustic emission method in [11-13]. In the elastic compliance method, a load was applied to

the specimen by a stepping motor and the displacement of the loading bar was fixed by locking the stepping motor. The load was continuously monitored by a load cell in line with the stepping motor. Crack extension increases the specimen compliance and therefore, results in a decrease in load for the fixed displacement.

The specimen compliance was also monitored for measuring the DHC growth rates in the axial direction of unirradiated tube #601. Two DHC growth rate tests were performed on each CCT specimen at two different temperatures. The specimen was heat tinted after the first test to mark the end of crack growth. Once both tests were finished the specimen was heat-tinted again and then broken apart. The fracture surface was photographed and the crack length was determined by dividing the fracture area by the specimen thickness. Finally, the DHC growth rates in the axial or radial directions were calculated by dividing the crack length by the growth test time, excluding the incubation time. In some DHC tests, there was a short standing time before the crack initiation, termed "incubation time". DHC growth rate tests were performed on 7 irradiated and 11 unirradiated CB specimens (in the radial direction) and 7 unirradiated CCT specimens (in the axial direction) at test temperatures of 80, 100, 120 and 130°C, respectively.

2.3 Threshold stress intensity, K_{IH} tests

The elastic compliance method was also used to measure the radial-axial threshold stress intensity factor, K_{IH}, for DHC initiation. The K_{IH} test was conducted following a DHC growth rate test, and therefore there was a sharp crack at the notch tip. The temperature cycle of the K_{IH} test was similar to the DHC growth rate test. The specimens were held for 1 hour at the peak temperature of 280°C before cooling to the test temperature of 100°C. The specimen was held at 100°C for half an hour before a load equivalent to a nominal K_I of 12 MPa√m at the crack tip was applied. After the load drop > 0.1N (to ensure crack initiation), the load was deceased to a reduction in K_I by 10%. Usually, the noise in the load cell readings is approximately ≤ 0.02 N (peak to peak) in the DHC rigs at a constant room temperature. A load drop > 0.05 N was defined as a crack initiation event. Once crack initiation was detected, the load was decreased to a reduction in K_I by 10% and the test continued with this reduced load until there was a further indication of crack initiation. Due to the uncertainty in the actual crack length, there was some uncertainty in the actual value of K_I. This process was repeated until the load did not drop by more than 0.02 N over one hundred hours. At the end of last stage the test was stopped since the consistency in the load indicated that there was no DHC initiation over four days. After the test finished, the specimen was heat-tinted then broken apart and then the fracture surface was photographed. All fracture surfaces were scrutinized on requirements similar to those specified in ASTM E1681, but slightly modified for DHC cracks due to the tendency for tunnelling. Some of the results were rejected based on this assessment. Finally, the threshold stress intensity factor K_{IH} was calculated using ASTM E1681 from the load at the last stage and total crack length.

2.4 Terminal Solid Solubility (TSS) of hydrogen tests

The initial hydrogen concentration of tube #601 is ~16μg/g, which TSSD (for hydride dissolution) temperature would be ~167°C. To determine TSS at the operation temperature

~100°C of the HEC pressure tube, it was necessary to reduce the hydrogen concentration. Three specimens were degassed in an ultra-high vacuum chamber (~10^{-8} torr, i.e. ~10^{-6} Pa) at temperatures of 550, 650 or 700°C, respectively. The specimens were held at a temperature for two hours before furnace cooling to room temperature. This treatment reduced the hydrogen concentration from ~16 μg/g to ~14, ~12 and ~9 μg/g with increasing annealing temperatures. Measurements of the dynamic elastic modulus as a function of temperature were conducted during thermal cycling using an internal friction instrument: the Automated Piezoelectric Ultrasonic Composite Oscillator Technique (APUCOT). The experimental procedure has been described in detail elsewhere [14-16]. For the degassed specimens the signal corresponding to the TSS temperature was weak due to the lower concentration of hydrogen. The uncertainty of TSS temperature was estimated to be ~ ±3°C, which is larger than the error of ±1°C in previous tests for as-received material [16]. Measurements of TSS at higher temperatures for Excel specimens doped with hydrogen were previously reported [14]. For irradiated materials, annealing for hydrogen extraction could vary the irradiated microstructure, thus the TSS tests were only performed in three coupons of tube #600 without degassing. The TSS temperatures in three irradiated coupons were determined using the Differential Scanning Calorimetry (DSC) technique [14]. After finishing the TSS measurements, the hydrogen concentrations in all specimens were analyzed using the HVEMS technique [17].

2.5 Elastic modulus tests

The Young's modulus as a function of temperature was determined in the axial and transverse directions of the unirradiated Excel pressure tube #601. Measurements of Young's modulus were conducted using an ultrasonic resonance technique [16]. The principle of elastic modulus measurements using the APUCOT is consistent with the sonic resonance technique in ASTM Standard E1875-00. The density of the Excel alloy was calculated from measurements of the specimen dimensions and mass. An average of 6.52 g/cm^3 was determined from all specimens with an error of ± 0.5%. The relative error of Young's modulus is ≤ ± 1% and the error of temperature measurements was ± 1°C.

3. Experimental results

3.1 DHC growth rates

A typical curve of load versus time during a DHC growth rate test at 80°C for CB specimen Ex-601-4 is shown in Fig. 3. For this specimen, a slow and small load drop following the initial load drop is thought to be the incubation period, and then the DHC initiated at the approximately 62nd hour, indicated by an arrow in Fig. 3. Once a crack initiates, then the load decreases at a constant rate, which is an indication that the DHC growth rate is constant despite the load reduction. This is consistent with the observation in Zr-2.5Nb, i.e. the DHC growth rate is insensitive to the applied stress intensity factor in stage II of V_r versus K_I curve [18]. The time of DHC growth is defined from the crack initiation to the end of the test excluding the incubation

time. A digital image of the fracture surface was taken, as shown in Fig. 4. The blue area is crack growth during the DHC growth rate test. The gold area corresponds to crack growth during the subsequent K_{IH} test, which will be described in the next section. The DHC growth rate tests in the axial direction were performed in CCT specimens at 80, 100, 120 and 130°C. A typical fracture surface of a CCT specimen is shown in Fig. 5, where dark blue and gold zones show the crack areas of two consecutive DHC growth rate tests, and the light blue zone is the pre-crack by fatigue cycling.

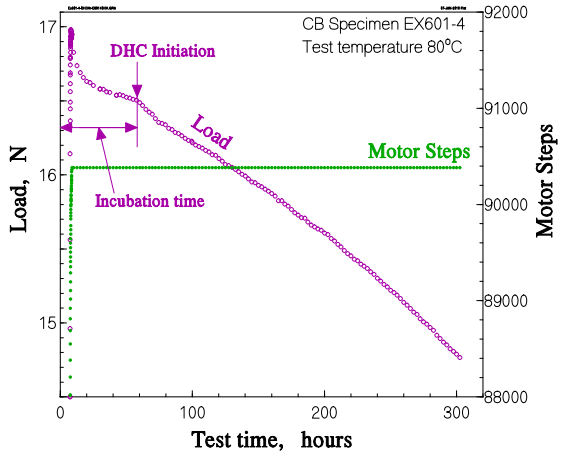

Fig. 3 DHC growth rate test in CB specimen EX601-4 shows the load drop vs. test time.

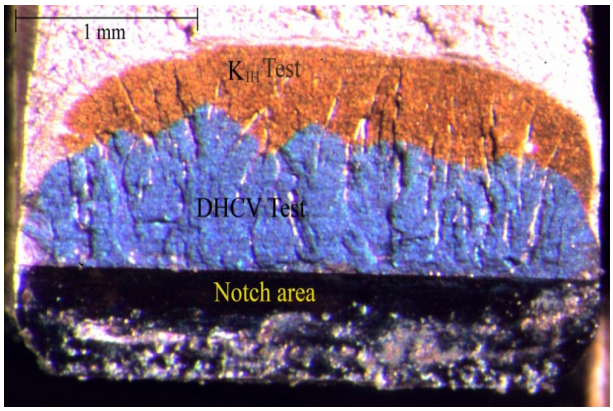

Fig. 4 Fracture surface of CB specimen EX601-4 shows two DHC crack zones.

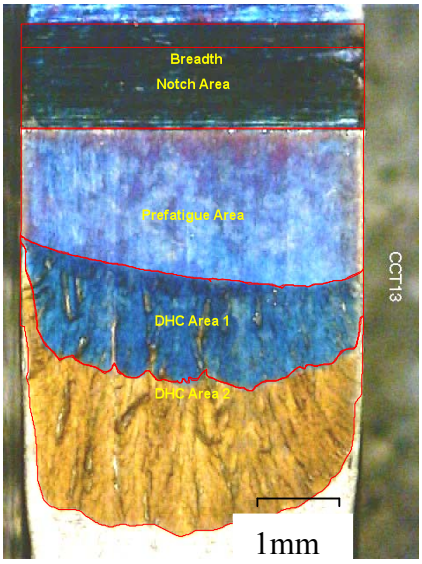

Fig. 5 Fracture surface of CCT specimen CCT-13 shows two DHC crack zones and a pre-crack by fatigue cycling.

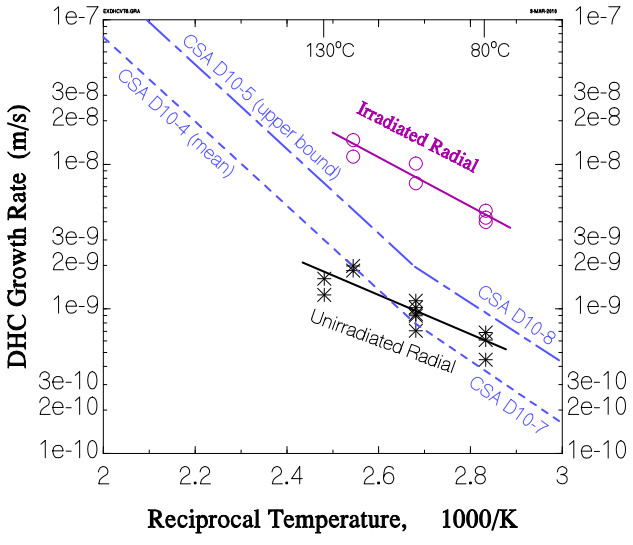

Fig. 6 DHC growth rate at the radial direction vs. the reciprocal temperature in Excel. Dashed lines show the mean and upper bound of Zr-2.5Nb.

Experimental results of the DHC growth rate in the radial direction for both unirradiated and irradiated Excel pressure tube material are shown in Fig. 6. DHC growth rates in the axial direction for unirradiated Excel pressure tube material are shown in Fig. 7. A least square, linear regression of the logarithm of DHC growth rate versus the reciprocal of temperature produced the following expressions:

$V_r = 2.6 \times 10^{-4} \exp(-32{,}139 / RT)$ for irradiated Excel in the radial direction (1)

$V_r = 4.4 \times 10^{-6} \exp(-26{,}208 / RT)$ for unirradiated Excel in the radial direction (2)

$V_a = 6.4 \times 10^{-6} \exp(-25{,}306 / RT)$ for unirradiated Excel in the axial direction (3)

where DHC growth rates V_r and V_a are in m/s, T is temperature in K, and R = 8.314 J/(K·mole). These equations are plotted using full lines in Figs. 6 and 7. For comparison, the mean and upper-bound equations of DHC growth rate for irradiated Zr-2.5Nb from Canadian Standard CSA N285.8-05 [19] are also included in these figures. The DHC growth rate for unirradiated Excel pressure tube material in the axial direction is higher than that in the radial direction. The DHC growth rate for irradiated specimens is higher than that for unirradiated specimens. The DHC growth rate of equation (1) for irradiated Excel is greater than the upper bound for irradiated Zr-2.5Nb as shown in Fig. 6. Furthermore, the neutron fluence ~ 2.8 x 10^{25} n/m^2 (E > 1 MeV) for tube #600 is below the saturation value for DHC growth rate in Zr-2.5Nb [20]. If a similar relationship between fluence and DHC growth rate is applicable for Excel, the DHC growth rate at higher fluences for Excel could be higher.

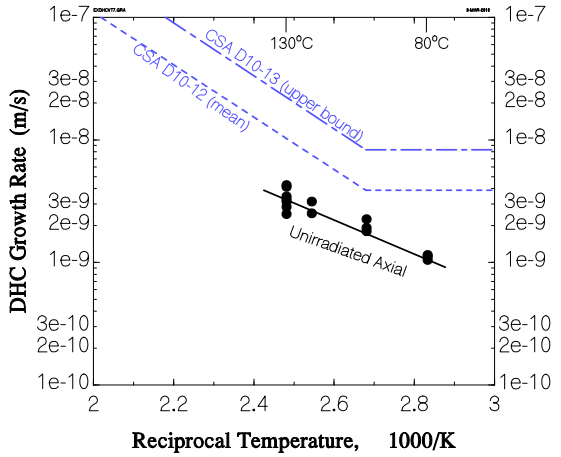

Fig. 7 DHC growth rate at the axial direction vs. 1/T in Excel. The dashed lines show the mean and upper-bound of Zr-2.5Nb.

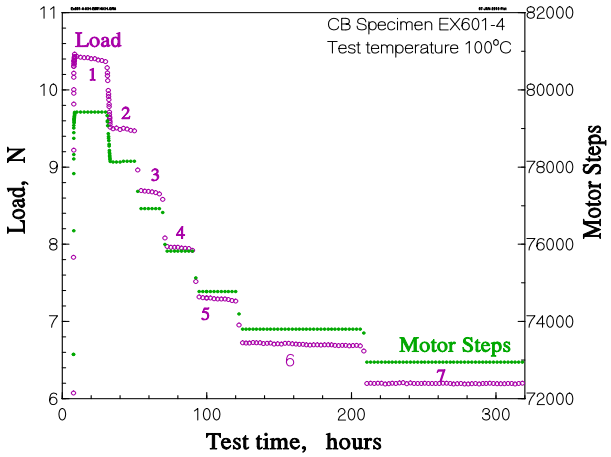

Fig. 8 K_{IH} test in CB specimen EX601-4 shows the load drop steps vs. test time. No load drop was detected in step No.7.

3.2 K_{IH}

The results from a representative K_{IH} test at 100°C for unirradiated Excel are shown in Fig. 8. During the first six stages of the test the load drop is large enough to ensure crack initiation. During the seventh, i.e. the final stage of the test, the fluctuation in load is ≤ 0.02 N. There was no evidence of DHC initiation in the final stage from 210 hr to 320 hr, which lasted more than 4 days. This load in the final stage determines the threshold stress intensity factor, K_{IH}. The total crack length was measured by the sum of gold and blue areas in Fig. 4. Results from K_{IH} tests for irradiated and unirradiated Excel pressure tube material are given in Table 1. An average and standard deviation of the data for five irradiated specimens and three unirradiated specimens are:

$$K_{IH} = (7.8 \pm 0.4)\ \text{MPa}\sqrt{\text{m}} \quad \text{for unirradiated Excel} \quad (4)$$

$$K_{IH} = (7.0 \pm 0.5)\ \text{MPa}\sqrt{\text{m}} \quad \text{for irradiated Excel} \quad (5)$$

Table 1 Experimental results of K_{IH} (MPa√m) in Excel at 100°C.

Sample	1846-6a	1846-6b	1846-7a	1846-8a	1846-8b	601-3	601-4	601-5
K_{IH}	7.6	7.5	6.4	6.9	6.7	8.3	7.9	7.2
Comments	Irradiated	Irradiated	Irradiated	Irradiated	Irradiated	Unirr.	Unirr.	Unirr.

Prior to this investigation there was no K_{IH} data at 100°C for annealed Excel. In the early 1980s Cheadle et al. [10,21] determined a K_{IH} range of 4.8 to 6 MPa√m at 137°C (410 K) for unirradiated 5% cold-worked (not annealed) Excel. Their values of K_{IH} are lower than the present value determined for annealed unirradiated Excel. The difference may be attributed to differences in the microstructure between cold worked and annealed pressure tubes. In the present measurements of K_{IH}, the lower value of 6.4 MPa√m for irradiated Excel is above the low-bound value of 4.5 MPa√m for Zr-2.5Nb given by Canadian Standard CSA N285.8-05[19].

3.3 TSS of hydrogen

For the unirradiated Excel specimens, the hydrogen concentration was 16 ± 1 μg/g, and the hydrogen concentration for the irradiated tube #600 was 20 ± 1 μg/g at the middle location. For the three irradiated coupons the measurements of TSS temperature is listed in Table 2 and shown in Fig. 9. Also included in this Figure and Table are results from three degassed specimens. Measurements of TSS temperatures in unirradiated Excel with higher concentrations of hydrogen were previously reported in [14]. The three equations of solubility limits given in [14] are:

$$C_H = 1.09 \times 10^5 \exp(-32{,}590/RT) \quad \text{for TSSD} \quad (6)$$

$$C_H = 1.45 \times 10^5 \exp(-29{,}930/RT) \quad \text{for TSSP2} \quad (7)$$

$$C_H = 1.43 \times 10^5 \exp(-30{,}680/RT) \quad \text{for TSSP1} \quad (8)$$

where C_H is hydrogen solubility in μg/g, T is temperature in K and R = 8.314 J/(K·mol). There are two equations for TSSP (for hydride precipitation) [14-16], because the TSSP is dependent on the maximum temperature (T_{max}) of thermal cycling. From that temperature (T_{max}), the specimen was cooled down and the TSSP was determined during this cooling. The TSSP1 characterizes the value of TSSP with a higher T_{max} > 410°C, while the TSSP2 represents the value of TSSP with a lower T_{max} (= TSSD temperature + 30°C). In the present work, the TSSD temperatures obtained in the three degassed specimens contain higher errors (± 3ºC) than previous measurements (± 1ºC) in [14,16]. The three data points of degassed specimens are located just above the extrapolated TSSD line of equation (6) in Fig. 9. For irradiated Excel, the TSS measurements, including three data points of TSSD and one TSSP, are slightly higher than the TSS lines given by equations from unirradiated material, Fig. 9. At the present, it cannot derive any new TSSD equation from only a few data. According to all experimental results the hydrogen solubility in Excel is approximately twice that in Zr-2.5Nb given by the Canadian Standard CSA N285.8-05 [19].

Table 2 Additional measurements of TSS temperature (°C) in irradiated or degassed Excel

Sample ID	1846-5a*	1846-5b	1846-5c	E601-0	E601-1	E601-2	E601-3
Hydrogen, (μg/g)	20±1	20±1	20±1	16.2±0.9	14.3±0.9	12.4±0.9	8.8±0.9
TSSD temperature	170.6±1	169.5±1	169.4±1	167.5±2	161±3	146±3	132±3
Comments	irradiated	irradiated	irradiated	unirradiat.	degassed	degassed	degassed

*Only TSSP temperature of 1846-5a was determined to be (114.5±1)°C with a T_{max}= 325°C.

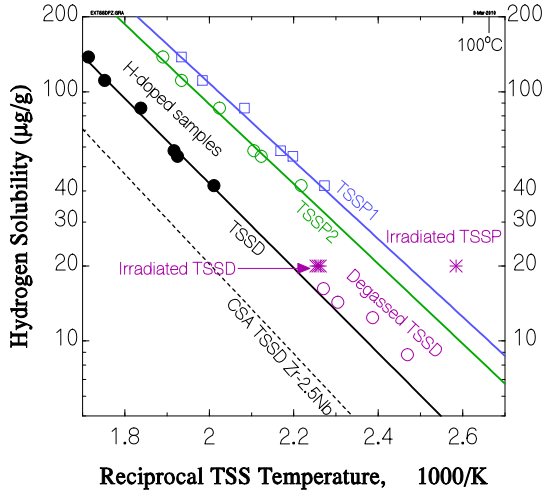

Fig. 9 Hydrogen solubility versus TSS temperature in Excel comparing with Zr-2.5Nb.

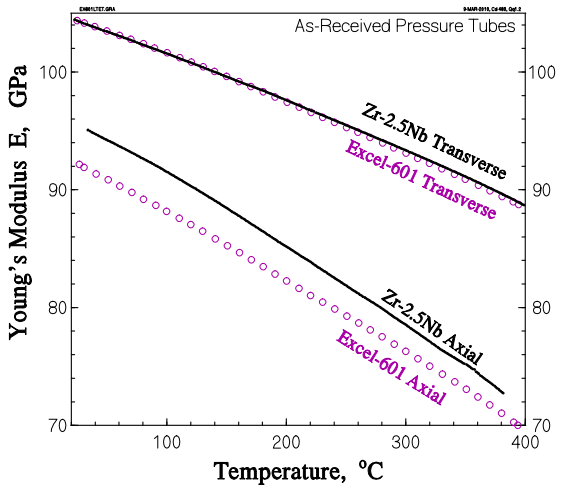

Fig. 10 Elastic modulus as a function of temperature in Excel and Zr-2.5Nb.

3.4 Elastic modulus

Two experimental curves of Young's modulus versus temperature in the axial and transverse directions of Excel tube #601 are shown in Fig. 10. Results for a Zr-2.5Nb pressure tube determined in the present work are included for comparison. It is shown that Young's modulus of the Excel in the transverse direction is coincident with that of Zr-2.5Nb over the temperature range from 20°C to 400°C, but in the axial direction, values of the Excel are slightly lower than (-6 % at 25°C or -4% at 380°C) the values of Zr-2.5Nb. The difference of ~6% in axial Young's modulus between the two Zr alloys is slightly larger than the measurement error of ± 1%. Curve-fits to the experimental data in Excel yield the following equations:

$$E = 93.64 - 0.05434T - 7.848 \times 10^{-6}T^2 - 1.407 \times 10^{-8}T^3 \quad \text{axial direction} \quad (9)$$

$$E = 105.24 - 0.03324T - 3.333 \times 10^{-5}T^2 - 3.09 \times 10^{-8}T^3 \quad \text{transverse direction} \quad (10)$$

where E is Young's modulus in GPa, T is temperature in °C, and the correlation coefficient is R^2 = 0.99993 and 0.99996, respectively.

4. Conclusions

DHC properties of annealed Excel are presented in the paper. Measurements of K_{IH} (for both unirradiated and irradiated material), DHC growth rate in the radial direction (for both materials), and DHC growth rate in the axial direction (unirradiated material) have been conducted at temperatures corresponding to the operating temperature range for the proposed Gen IV (SCWR) CANDU pressure tube design. It was found that:

(1) The radial-axial threshold stress intensity factor, K_{IH}, for DHC in irradiated Excel pressure tube material is higher than the lower bounds for ex-service Zr-2.5Nb pressure tube material.

(2) The DHC growth rate in Excel pressure tube material is greater than in Zr-2.5Nb at temperatures between 80 and 130°C.

(3) The solubility of hydrogen in Excel is roughly twice that in Zr-2.5Nb.

(4) The elastic modulus of unirradiated Excel is close to that of Zr-2.5Nb from room temperature to 400°C.

5. Acknowledgements

The author would like to thank Dr. C.K. Chow and M. Resta Levi, who were involved with this investigation in the early stages and contributed many valuable suggestions and to thank Dr. S. St. Lawrence and H. Chaput for their review of the manuscript. The work was partially funded by Natural Resources Canada, Next Generation Nuclear Portfolio Project with a project number Gen IV-FC-032026.

6. References

[1] D.F. Torgerson, B.M. Shalaby and S. Pang, "CANDU Technology for Generation III+ and IV Reactors", Nuclear Engineering and Design, Vol. 236 (2006), pp. 1565-1572.

[2] A Technology Roadmap for Generation IV Nuclear Energy Systems, Generation IV International Forum, GIF-002-00, December, 2002.

[3] C.K. Chow, S.J. Bushby and H.F. Khartabil, "A Fuel Channel Design for CANDU-SCWR", *Proceedings of ICONE 14, 14TH International Conference on Nuclear Engineering*, July, 2006, Miami, Florida, USA, ASME 2006, paper ICONE14-89678.

[4] C.K. Chow and H.F. Khartabil, "Conceptual Fuel Channel Designs for CANDU-SCWR", Nucl. Eng. & Technology, Special Issue on the 3rd International Symposium on SCWR, Vol.40, No.2 (2008), pp.139-146.

[5] H.F. Khartabil, R.B. Duffey, N. Spinks and W. Diamond, "The Pressure-Tube Concept of Generation IV Supercritical Water Cooled Reactor (SCWR): Overview and Status", *Proceedings of ICAPP' 05*, Seoul, Korea, May, 2005, paper 5564.

[6] R.B. Duffey, I.L. Pioro, B.A. Gabaraev and Yu.N. Kuznetsov, "SCW Pressure-Channel Nuclear Reactors: Some Design Features and Concepts", *Proceedings of ICONE 14, 14TH International Conference on Nuclear Engineering*, July, 2006, Miami, Florida, USA, ASME 2006, paper ICONE14-89609.

[7] B.A. Cheadle, R.A. Holt, V. Fidleris, A.R. Causey and V.F. Urbanic, "High Strength, Creep-Resistant Excel Pressure Tubes", *5th International Symposium on Zirconium in Nuclear Industry*, ASTM, STP 754, ASTM International, 1982, pp. 193-207.

[8] B.A. Cheadle and R.A. Holt, U.S. Patent 4 452 648 "Low in Reactor Creep Zr Base Alloys", June 5, 1984.

[9] E,F, Ibrahim and B.A. Cheadle, "Development of Zirconium Alloy for Pressure Tubes in CANDU Reactors", Can. Met. Quart., Vol.24 (1985) p.273.

[10] C.E. Ells, C.E. Coleman, B.A. Cheadle, S. Sagat, D.K. Rodgers, "The Behaviour of Hydrogen in Excel Alloy", J. Alloy Comp. Vol. 231 (1995), pp. 785 – 791.

[11] S. Sagat, C.E. Coleman, M. Griffiths and B.J.S. Wilkins, "The Effect of Fluence and Irradiation Temperature on Delayed Hydride Cracking in Zr-2.5Nb", *10th International Symposium on Zirconium in Nuclear Industry*, ASTM STP 1245, A.M. Grade and E.R. Bradley, Eds, ASTM International, West Conshohocken, PA, 1994, pp.35-61.

[12] S. Sagat and M.P. Puls, "Temperature Limit for Delayed Hydride Cracking in Zr-2.5Nb Alloys", *Transaction of the 17th International Conference on Structure Mechanics in Reactor Technology (SMiRT 17)*, Prague, Czech, August, 2003, Paper #G06-4.

[13] M. Resta Levi and M.P. Puls, "DHC behaviour of irradiated Zr-2.5Nb Pressure Tubes up to 365°C", *Transaction of the 18th International Conference on Structure Mechanics in Reactor Technology (SMiRT 18)*, Beijing, China, August, 2005, Paper #G10-3.

[14] D. Khatamian, Z.L. Pan, M.P. Puls and C.D. Cann, "Hydrogen Solubility Limits in Excel, an Experimental Zirconium-Based Alloy", J. Alloys & Compounds, Vol. 231, (1995), pp. 488-493.

[15] Z.L. Pan, M.P. Puls and I.G. Ritchie, "Measurements of Hydrogen Solubility during Isothermal Charging in a Zr Alloy using an Internal Friction Technique", J. Alloys & Compounds, Vol. 211/212 (1994), pp. 245-248.

[16] Z.L. Pan, I.G. Ritchie, and M.P. Puls, "The Terminal Solid Solubility of Hydrogen and Deuterium in Zr-2.5Nb Alloys", J. Nucl. Mat. Vol.228, (1996), pp. 227-237.

[17] G.A. Bickel, L.W. Green, M.W.D. James, T.G. Lamarche, P.K. Leeson and H. Michel, "The Determination of Hydrogen and Deuterium in Zr-2.5Nb Material by Hot Vacuum Extraction Mass Spectrometry", J. Nucl. Mat. Vol. 306 (2002) p.21

[18] A. Sawatzky and C.E. Ells, "Understanding Hydrogen in Zirconium", *12th International Symposium on Zirconium in Nuclear Industry*, Eds. By G.P. Sabol and G.D. Moan, ASTM STP 1354, ASTM International, West Conshohocken, PA, 2000, pp.32 – 48.

[19] Canadian Standard Association, "Technical Requirements for In-Service Evaluation of Zirconium Alloy Pressure Tubes in CANDU Reactors", CSA N285.8-05, 2005, p. 173.

[20] Z.L. Pan, S. St Lawrence, P.H. Davies, M. Griffiths and S. Sagat, "Effect of Irradiation on the Fracture Properties of Zr-2.5Nb Pressure Tube at the End of Design Life", *14th International Symposium on Zirconium in Nuclear Industry*, ASTM STP 1467, J. ASTM International, Vol. 2 (2005) No.9, pp.759 – 780.

[21] B.A. Cheadle and C.E. Coleman, "Delayed Hydride Cracking in a Strong Creep Resistant Zirconium Alloy", Trans. Jap. Inst. Metals, Vol. 21, (1980), pp. 517-520.